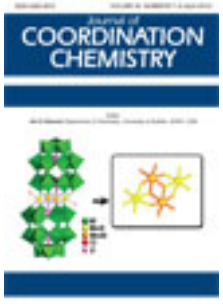


Journal of Coordination Chemistry
Publication details, including instructions for authors and subscription information:
http://www.tandfonline.com/loi/gcoo20

# Synthesis, characterization, and polyphenol oxidase activity of $Cu^{II}$, $Mn^{II}$, and $Fe^{III}$ complexes with a $N_2O_2$ ligand

Lijun Lu [a] , Yanying Song [a] , Hui Liu [a] & Jingyan Zhang [a]
[a] State Key Laboratory of Bioreactor Engineering, Department of Pharmaceutical Sciences , School of Pharmacy, East China University of Science & Technology , Shanghai 200237 , P.R. China
Published online: 21 Mar 2012.

To cite this article: Lijun Lu , Yanying Song , Hui Liu & Jingyan Zhang (2012) Synthesis, characterization, and polyphenol oxidase activity of $Cu^{II}$, $Mn^{II}$, and $Fe^{III}$ complexes with a $N_2O_2$ ligand, Journal of Coordination Chemistry, 65:7, 1278-1288, DOI: 10.1080/00958972.2012.671480

To link to this article: http://dx.doi.org/10.1080/00958972.2012.671480

*Journal of Coordination Chemistry*
Vol. 65, No. 7, 10 April 2012, 1278–1288



# Synthesis, characterization, and polyphenol oxidase activity of $Cu^{II}$, $Mn^{II}$, and $Fe^{III}$ complexes with a $N_2O_2$ ligand

LIJUN LU, YANYING SONG, HUI LIU and JINGYAN ZHANG*

State Key Laboratory of Bioreactor Engineering, Department of Pharmaceutical Sciences, School of Pharmacy, East China University of Science & Technology, Shanghai 200237, P.R. China

(*Received 17 October 2011; in final form 3 February 2012*)

To explore the effect of the metal center on catechol oxidase and tyrosinase activities, four complexes, $Cu_2(\mu\text{-}Cl)_2(hbpg)_2$ (**1**), $[Cu_2(\mu\text{-}OH_2)_2(hbpg)_2](NO_3)_2(H_2O)_2$ (**2**), $[Fe_2(\mu\text{-}Cl)_2(hbpg)_2]Cl_2(H_2O)_2$ (**3**), and $[Mn_2(\mu\text{-}Cl)_2(hbpg)_2](H_2O)_2$ (**4**) (hbpg = *N*-(2-hydroxybenzyl)-*N*-(2-picolyl)glycine), were synthesized and characterized with elemental analysis, single-crystal X-ray diffraction, molar conductivity measurements, mass spectrometry, UV-Visible, and FT-IR spectroscopies. The X-ray crystal structural analysis indicates that **1** has a binuclear copper, coordinated with $N_2O_2$ ligands. Complementary characterizations suggested that **2**, **3**, and **4** have similar coordination sphere. Complex **3** exhibits much higher catechol oxidase and tyrosinase-like activity than **1**, **2**, and **4**. The results suggested that with a similar coordination sphere, the redox potential of the metal center is critical for catalytic activity. This work provides valuable information for improving the polyphenol oxidase activity of metal complexes for phenolic degradation.

*Keywords*: Metal complexes; Catechol oxidase; Tyrosinase; Redox potential



## 1. Introduction

Polyphenol oxidase is a category of metalloenzymes which can catalyze the hydroxylation of phenols to quinones by molecular oxygen [1–3]. Typical examples in this category of enzymes are catechol oxidase and tyrosinase, the former catalyzes exclusively the oxidation of catechol, while the latter shows cresolase activity (phenols to *o*-diphenols) as well as catecholase activity (*o*-diphenols to *o*-quinones) [4, 5]. Both are typical type III copper enzymes, in which the active site is a binuclear copper center. To understand the mechanisms of enzymes and mimic their catalysis, a large number of model complexes of these enzymes have been prepared and studied [6–15]. Studies of the model complexes indicated that the distance of the two coppers in binuclear complexes is critical to their catalytic activities [16, 17]. Some researchers also believed that the redox potential of the complexes and their catalytic activities are closely related [18, 19]. However, the complexity of the redox potential of the multinuclear complexes hinders direct correlation between the redox potential and activity of the complexes.

*Corresponding author. Email: jyzh04@yahoo.com


ISSN 0095-8972 print/ISSN 1029-0389 online 
http://dx.doi.org/10.1080/00958972.2012.671480

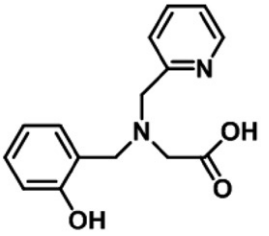


Figure 1. The structure of *N*-(2-hydroxybenzyl)-*N*-(2-picolyl) glycine.



Manganese and iron are also found at the active site of many highly efficient oxidases and oxygenases [20–24]. Since they are also redox active as is copper, it will be interesting to compare the catalytic activity of the complexes with a similar coordination sphere and metal ions with different redox potentials. The activity difference between these complexes may shed light into the relationship between redox potential of complexes and their catalytic activity.

In this study, we synthesized four binuclear copper, manganese, and iron complexes with *N*-(2-hydroxybenzyl)-*N*-(2-picolyl) glycine ligand. The ligand is chosen for its coordination mode quite similar to copper, manganese, and iron ions; the structure of the ligand is shown in figure 1. The metal complexes with the ligand were systematically characterized with UV-Visible spectroscopy, FT-IR spectroscopy, single-crystal X-ray diffraction, molar conductivity, mass spectrometry (MS), and elemental analysis. Catechol oxidase and tyrosinase activities of the synthesized complexes were compared. We believe the activity difference of the four complexes originated from their metal centers, which have different redox potentials.

## 2. Experimental

### 2.1. *Materials*

All reagents and organic solvents were of reagent grade and used as received. Pyridine-2-carboxaldehyde, 3,5-di-tert-butylcatechol (3,5-DTBC), and 2,6-dimethoxyphenol (2,6-DMP) were purchased from Alfa Aesar Company, and other reagents were purchased from SinoPharm Chemical Reagent Co., Ltd.

### 2.2. *Physical measurements*

$^1$H NMR spectra were recorded on an AVANCE 500 analyzer (Bruker, Germany). Electronic spectra were obtained on a Cary 50 spectrophotometer (Varian, USA). Infrared (IR) spectra were measured on a Perkin-Elmer FT-IR 1760-X (KBr pellets, 4000–400 $cm^{-1}$). Elemental analyses were performed with an Elemental Vario ELIII analyzer (Germany). X-ray crystallographic data of the complexes were collected on a SMART diffractometer (Bruker, USA) using Mo-K$\alpha$ radiation ($\lambda = 0.71073$ Å). MS data were obtained with an Esquire 3000 (Bruker, USA). Conductivity measurements were carried out with an HI8733 conductivity meter using methanol as solvent.

### 2.3. *Synthesis*

**2.3.1. Ligand synthesis.** The ligand *N*-(2-hydroxybenzyl)-*N*-(2-picolyl)glycine (hppg) was synthesized in two steps using the literature procedure with a slight modification [1]. First, *N*-(2-hydroxybenzyl)glycine was synthesized. Glycine (1.20 g, 16 mmol) and sodium hydroxide (0.64 g, 16 mmol) were dissolved in 20 mL of $H_2O$, then one equivalent of salicylaldehyde (1.92 g, 16 mmol) in ethanol was added. After 30 min of stirring, $NaBH_4$ (0.75 g, 20 mmol) was slowly added to the yellow mixture in an ice bath. After the addition of $NaBH_4$, the reaction mixture turned into a white and turbid solution. The solution was filtered and the supernatant was acidified to pH 4 with concentrated hydrochloric acid after overnight stirring. White solid was formed when the reaction mixture was cooled to 0°C, and was collected by filtration and washed with a small amount of cold water and ethanol. White powder was obtained with a yield of 76% (2.20 g); m.p. = 221–222°C.

One equivalent of sodium hydroxide (0.40 g, 10 mmol) was added to the prepared *N*-(2-hydroxybenzyl)glycine (1.81 g, 10 mmol), then one equivalent of pyridine-2-carboxaldehyde (10 mmol, 0.56 g) was added dropwise, yielding a clear yellow solution. After 2 h of stirring, $NaBH_4$ (0.49 g, 13 mmol) was slowly added in an ice bath, then stirred for another 12 h at room temperature. The solution was acidified to pH 4 with concentrated acetic acid. A white solid precipitate was obtained after a short while. The solid was collected by filtration, with a yield of 47% (1.29 g). $^1$H NMR ($D_2O$): 8.50 (d, $J = 4.68$ Hz, 1H, pyridine), 8.03 (t, $J = 7.8$ Hz, 1H, pyridine), 7.55 (t, $J = 4.69$ Hz, 2H, pyridine), 7.16 (m, 2H, ArH), 6.81 (t, $J = 7.46$ Hz, 1H, ArH), 6.69 (d, $J = 8.11$ Hz, 1H, ArH), 4.41 (s, 2H, N–$CH_2$–pyridine), 4.21 (s, 2H, N–$CH_2$–Ar), 3.80 (s, 2H, N–$CH_2$–$CO_2$).

**2.3.2. Synthesis of $Cu_2(\mu\text{-}Cl)_2(hbpg)_2$ (1).** $CuCl_2 \cdot 2H_2O$ (0.0861 g, 0.5 mmol) in 5 mL water was added to a 10 mL aqueous solution of hppg (0.1362 g, 0.5 mmol) with stirring. Blue solid was precipitated instantly. The resulting mixture was allowed to react further for 2 h and the blue solid was collected and re-crystallized from water. Yield: 71% (0.1311 g). Anal. Calcd (%): C, 48.65; N, 7.57; H, 4.08. Found (%): C, 48.26; N, 7.27; H, 3.92. Crystal of **1** was obtained by keeping its methanol solution at room temperature for several days.

**2.3.3. Synthesis of $[Cu_2(\mu\text{-}OH_2)_2(hbpg)_2](NO_3)_2(H_2O)_2$ (2), $[Fe_2(\mu\text{-}Cl)_2(hbpg)_2]Cl_2(H_2O)_2$ (3), $[Mn_2(\mu\text{-}Cl)_2(hbpg)_2](H_2O)_2$ (4).** Complexes **2**–**4** were synthesized with the same procedure as **1** except that the metal sources were $Cu(NO_3)_2 \cdot 3H_2O$, $FeCl_3 \cdot 6H_2O$, and $MnCl_2 \cdot 4H_2O$, respectively. $[Cu_2(\mu\text{-}OH_2)_2(hbpg)_2](NO_3)_2(H_2O)_2$ (**2**): Yield: 37% (0.0686 g). Anal. Calcd (%): C, 41.57; N, 9.70; H, 4.39. Found (%): C, 41.53; N, 9.76; H, 4.36. $[Fe_2(\mu\text{-}Cl)_2(hbpg)_2]Cl_2(H_2O)_2$ (**3**): Yield: 64% (0.1278 g). Anal. Calcd (%): C, 43.26; N, 6.73; H, 4.09. Found (%): C, 43.37; N, 6.21; H, 4.11. $[Mn_2(\mu\text{-}Cl)_2(hbpg)_2](H_2O)_2$ (**4**): Yield: 49% (0.8012 g). Anal. Calcd (%): C, 47.56; N, 7.40; H, 4.23. Found (%): C, 47.55; N, 7.34; H, 4.53.

### 2.4. *Catalytic activity assay*

The kinetic experiments were conducted at room temperature. Initial reaction rates were determined by linearly fitting the curve of the absorbance *versus* reaction time. In a typical oxidation reaction, 50 μL substrate solution, 10 μL of 10 mmol $L^{-1}$ metal complex aqueous, and 940 μL buffer solution were quickly mixed thoroughly. The final concentration of the metal complex was 0.1 mmol $L^{-1}$, 3,5-DTBC was 10 mmol $L^{-1}$, and 2,6-DMP was 100 mmol $L^{-1}$. The pseudo first-order condition was maintained by keeping the concentration of the substrate at least 10 times larger than that of the metal complex. For calculating $K_m$ and $V_{max}$, 3,5-DTBC solution with different concentrations (2.5–80 mmol $L^{-1}$) and 2,6-DMP (5–900 mmol $L^{-1}$) were used. The absorbances of 3,5-DTBQ and 2,6-DMQ were monitored at 410 and 478 nm, respectively.

## 3. Results and discussion

### 3.1. *Structural determinations of 1–4*

X-ray crystal structural analysis indicates that **1** is binuclear. Each copper is coordinated by two nitrogen atoms and two oxygen atoms from the ligand; two coppers are bridged by chloride in a double $\mu_2$-fashion. The coordination of $Cu^{2+}$ can be described as distorted octahedral; its ORTEP view is shown in figure 2. The crystallographic data and details of the refinement of the crystal structure of **1** are summarized in table 1. Selected bond distances and angles are listed in table 2. The Cu–O (carboxylate) (1.952(2) Å), Cu–N (pyridine) (1.995(3) Å), and Cu–N (amino) (2.044(3) Å) distances are comparable with those of the reported copper complexes [25]. The Cu–O (phenoxido) distance (2.541(3) Å) is relatively longer than that in many copper complexes [26], and thus we believe phenoxido is weakly bound to the copper [27].

In spite of many attempts, we were unable to obtain single crystals of **2**–**4**. Hence, the molar conductances of **1**–**4** were measured to assist in identifying their structures. According to the literature [28], for 2 : 1 electrolytes in methanolic solution at room

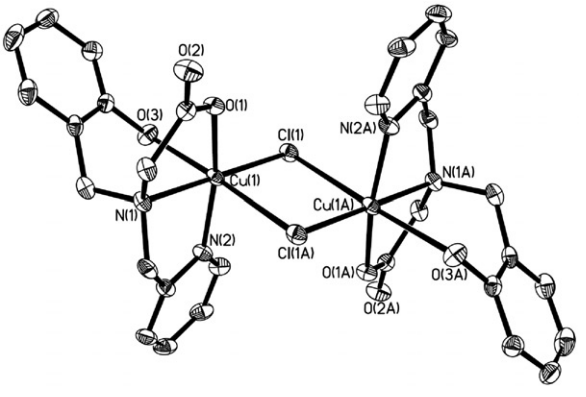


Figure 2. ORTEP view (30% probability thermal ellipsoids) of **1**.

temperature, the conductance is roughly ~160–220 s cm$^2$ mol$^{-1}$; for 1 : 1 electrolytes the conductance is 80–115 s cm$^2$ mol$^{-1}$; for non-electrolytes, conductance is below 80 s cm$^2$ mol$^{-1}$. Under the same conditions, the molar conductances of **1**, **2**, **3**, and **4** in methanol are 79, 212, 192, and 78 s cm$^2$ mol$^{-1}$, respectively. Thus **2** and **3** are 2 : 1 electrolytes, consistent with the formulas we proposed based on the elemental analysis. Conductance values of **1** and **4** are very close to that of the 1 : 1 electrolytes, perhaps because of the weakly bound phenoxide in these two complexes as we suggested from the Cu–O bond length.

Electrospray ionization-mass spectrometry (ESI-MS) was used to further determine the structures of **2**–**4**. For **2**, a peak at 704 $m/z$ was observed, which can be assigned as the cation $[Cu_2(\mu\text{-}OH)(\mu\text{-}OH_2)(hbpg)_2]^+$. The isotope peak caused by copper was also observed. One bridged proton in $H_2O$ possibly was removed during ionization. For **3**,



Table 1. Crystallographic parameters for $Cu_2(\mu\text{-}Cl)_2(hbpg)_2$ (**1**).

| | |
|---|---|
| Empirical formula | $C_{30}H_{30}Cl_2Cu_2N_4O_6$ |
| Formula weight | 740.58 |
| Temperature (K) | 293(2) |
| Wavelength (Å) | 0.71073 |
| Crystal system | Monoclinic |
| Space group | $P2_1/n$ |
| Unit cell dimensions (Å, °) | |
| $a$ | 13.711(3) |
| $b$ | 7.2070(14) |
| $c$ | 16.321(3) |
| $\beta$ | 111.62(3) |
| Volume (Å$^3$), $Z$ | 1499.3(5), 2 |
| Calculated density (Mg m$^{-3}$) | 1.640 |
| Absorption coefficient (mm$^{-1}$) | 1.648 |
| $F$(000) | 952 |
| Crystal size (mm$^3$) | 0.23 × 0.12 × 0.08 |
| $\theta$ range for data collection (°) | 3.13–25.50 |
| Reflections collected | 8662 |
| Independent reflection | 2789 [$R$(int) = 0.0505] |
| Completeness to $\theta$ = 25.50 (%) | 99.9 |
| Data/restraints/parameters | 2789/0/203 |
| Goodness-of-fit on $F^2$ | 1.032 |
| Final $R$ indices | $R_1$ = 0.0427, $wR_2$ = 0.0820 |
| $R$ indices (all data) | $R_1$ = 0.0592, $wR_2$ = 0.0875 |
| Largest difference peak and hole (e Å$^{-3}$) | 0.297 and −0.312 |

Table 2. Selected bond lengths (Å) and angles (°) for **1**.

| | | | |
|---|---|---|---|
| Cu(1)–O(1) | 1.952(2) | Cu(1)–Cl(1) | 2.244(1) |
| Cu(1)–N(2) | 1.995(3) | Cu(1)–O(3) | 2.541(3) |
| Cu(1)–N(1) | 2.044(3) | Cu(1)–Cl(1A) | 2.931(1) |
| O(1)–Cu(1)–N(2) | 165.67(10) | N(1)–Cu(1)–Cl(1) | 179.44(8) |
| O(1)–Cu(1)–N(1) | 83.44(10) | O(1)–Cu(1)–O(3) | 92.22(9) |
| N(2)–Cu(1)–N(1) | 82.46(11) | N(2)–Cu(1)–O(3) | 89.68(10) |
| O(1)–Cu(1)–Cl(1) | 97.02(8) | N(1)–Cu(1)–O(3) | 87.36(10) |
| N(2)–Cu(1)–Cl(1) | 97.10(9) | Cl(1)–Cu(1)–O(3) | 92.30(7) |
| Cl(1)–Cu(1)–Cl(1A) | 90.82(3) | O(3)–Cu(1)–Cl(1A) | 176.86(7) |
| Cu(1)–Cl(1)–Cu(1A) | 89.18(3) | | |

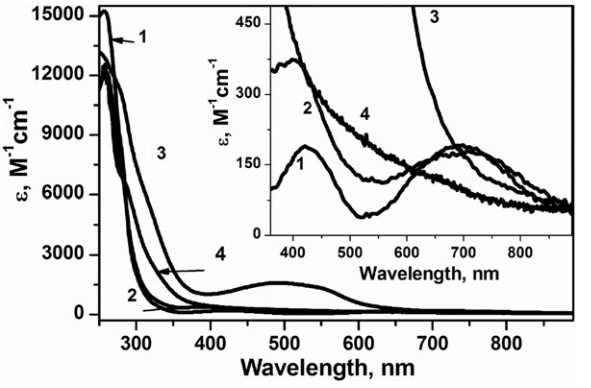


Figure 3. UV-Visible absorption spectra of **1–4**.



a peak at 381 $m/z$ assigned as $[Fe_2(\mu\text{-Cl})_2(hbpg)_2]^{2+}$ was observed. Since for **3**, the isotope peaks are not definitive due to peak overlapping, to determine the anions of **3** and **4** as we proposed according to the elemental analysis, silver nitrate was used. Adding silver nitrate to aqueous solutions of **3** and **4**, white precipitate was observed in the solution of **3**, but not in the solution of **4**, indicating that the anion in **3** is chloride. The result is consistent with the elemental analysis and conductivity. In **4**, a peak at 688 $m/z$ suggests that it is $[Mn_2(\mu\text{-Cl})(hbpg)_2]^{+}$, confirmed by the corresponding isotope peak of chlorine at 690 $m/z$. The fragments with anion were not observed in MS spectra of the complexes. These results further support elemental analyses.

To confirm the coordination spheres of **2–4** are similar to that of **1**, UV-Visible spectra of **1–4** were recorded (figure 3). The band at 260 nm in all the complexes is ascribed to the transition from the hppg itself. The bands at ~710 nm (in **1** and **2**) are assigned to copper d–d transitions in octahedral geometry [29, 30]. The bands at 420 nm occurring in copper complexes (**1** and **2**) and ~510 nm (in **3**) are caused by the ligand-to-metal ion charge-transfer [31, 32]. The UV-Vis spectra of **1** and **2** are quite similar as they have the same coordination sphere except for anion. There is no band between 300 and 800 nm in manganese complex **4** [33].

The FT-IR spectra of **1–4** showed typical broad bands from 3440 to 3425 $cm^{-1}$ due to $\nu$(OH) of water ligands. A couple of prominent bands at 1600–1290 $cm^{-1}$ were assigned to C=O, C=N, C=C, and C–O/phenolate stretching modes. These stretching modes in the four complexes are almost identical, indicating that the ligand in the different complexes coordinates in a similar mode. IR vibrations of the four complexes are detailed in table S1.

Based on elemental analyses, molar conductivity, ESI-MS, FT-IR, and UV-Visible spectra, we assume that **1–4** are quite similar in ligand coordination. Each metal ion is six coordinate by two nitrogen atoms and two oxygen atoms from the ligand and two anions or water molecules. Two metals in **1**, **3**, and **4** are bridged by two chlorides and copper centers are bridged by two water molecules in **2** (figure S1). In all complexes, the carboxylate coordinates monodentate, possibly because the bond angle of N(1)–C(27)–C(22) (111° in **1**) has to be very small to allow two oxygen atoms of carboxylate to be close to the metal ions, which are sterically crowded.

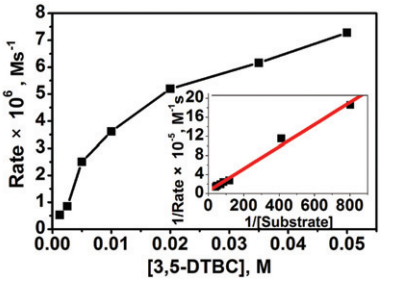


Figure 4. Plot of 3,5-DTBC oxidation reaction rates *vs.* concentration of 3,5-DTBC using **4** as catalyst. Inset: Lineweaver–Burk plot.

Table 3. Kinetic parameters for **1**, **3**, and **4** using 3,5-DTBC as substrate.

| Complex | $V_{max}$ (mmol $L^{-1}$ $s^{-1}$) | $K_m$ (mmol $L^{-1}$) | $K_{cat}$ ($h^{-1}$) | $K_{cat}/K_m$ ($h^{-1}$(mol $L^{-1}$)$^{-1}$) |
|---|---|---|---|---|
| **1** | $1.08 \times 10^{-2}$ | 31.59 | 390.2 | $1.24 \times 10^4$ |
| **3** | $1.30 \times 10^{-2}$ | 34.47 | 468.7 | $1.36 \times 10^4$ |
| **4** | $1.06 \times 10^{-2}$ | 24.67 | 381.6 | $1.55 \times 10^4$ |

### 3.2. *Catechol oxidase activity*

The catechol oxidase activities of **1**–**4** were studied with 3,5-DTBC as substrate. 3,5-DTBC has low quinone-catechol reduction potential and can be easily oxidized to the corresponding *o*-quinone, 3,5-DTBQ, which is stable and shows maximum absorption at 410 nm, such that the reaction can be easily followed spectrophotometrically. Through monitoring the absorbance of 3,5-DTBQ at 410 nm, the activities of **1**–**4** were compared. The activities of **1** and **2** are very similar; only the data of **1** is presented.

When the substrate was at low concentration, a first-order dependence of the reaction rate to substrate concentration was found. All complexes displayed saturation kinetics at high substrate concentrations. Figure 4 presents the dependence of the initial reaction rate on concentration of 3,5-DTBC using **4** as catalyst. $K_m$ and $V_{max}$ were obtained from the Lineweaver–Burk double reciprocal plot. The Lineweaver–Burk plots for **1** and **3** are provided in figure S2. Maximum velocity $V_{max}$, $K_{cat}$, and $K_m$ of the complexes were obtained from these plots and the data summarized in table 3. $K_m$ and $V_{max}$ of the three complexes are quite similar, while $K_{cat}$ of **3** is higher than the other two, indicating that **3** has higher catechol oxidase activity.

### 3.3. *Tyrosinase activity*

Similar to the catechol oxidase activity, tyrosinase activities of the four complexes were investigated using 2,6-dimethoxyphenol (2,6-DMP) as substrate. Because the tyrosinase activities of these four complexes are much lower than their catechol oxidase activities, the catalytic reaction condition was first optimized. The initial try showed that the catalytic activities of the complexes were solvent dependent. The formation of product

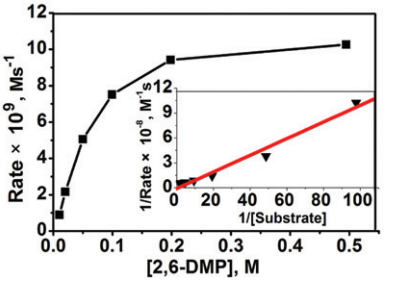


Figure 5. Plot of 2,6-DMP oxidation reaction rates *vs.* concentration of 2,6-DMP using **4** as catalyst. Inset: Lineweaver–Burk plot.



Table 4. Kinetic parameters for **1**, **3**, and **4** using 2,6-DMP as substrate.

| Complex | $V_{max}$ (mmol $L^{-1}$ $s^{-1}$) | $K_m$ (mmol $L^{-1}$) | $K_{cat}$ ($h^{-1}$) | $K_{cat}/K_m$ ($h^{-1}$(mol $L^{-1}$)$^{-1}$) |
|---|---|---|---|---|
| **1** | $1.78 \times 10^{-5}$ | 413 | 0.64 | 1.55 |
| **3** | $7.31 \times 10^{-5}$ | 170 | 2.63 | 15.47 |
| **4** | $1.78 \times 10^{-5}$ | 133 | 0.61 | 4.59 |

in acetonitrile is much faster than that in water for the first 10 min of the reaction, which may be due to better solubility of **1** in acetonitrile (figure S3A). However, the substrate conversion in water is the highest; there is no obvious substrate conversion in acetonitrile from 10 min to 12 h of the reaction (figure S3B). The effect of pH on the substrate conversion was also investigated. Figure S4 shows reactions of 2,6-DMP with **1** in solutions with different pH values for 2 h. Basic solutions should be favorable for phenol deprotonation during its oxidation and at pH 8, the reaction is fastest. Hence the catalytic reactions of the four complexes with 2,6-DMP were studied in pH 8 aqueous solution. Figure 5 presents the dependence of the initial reaction rate on the concentration of 2,6-DMP using **4** as catalyst. Table 4 summarizes the catalytic parameters using **1**, **3**, and **4** as catalysts. The higher $K_m$ of **1** is possibly due to steric effects. The catalytic ability order **3** > **1**(**4**) is consistent with their catechol oxidase activities.

Several factors need to be considered in assessing the difference in catalytic activities of **1**, **3**, and **4**, such as electrochemical properties, exogenous donors, and steric match. The ligand coordination in these complexes is quite similar, substrate binding sites are alike, and thus the steric match should cause less effect on catalytic activity. The catalytic difference, therefore, may correlate to electrochemical properties of the metal centers. The standard redox potentials of the three metals are quite different: $Fe^{3+}/Fe^{2+}$ (0.771 V), $Cu^{2+}/Cu^{+}$ (0.153 V), and $Mn^{3+}/Mn^{2+}$ (1.51 V) [34]. Higher reduction potential means the metal ion is easier to be reduced. According to this theory, the iron complex **3** should be more active than copper complexes **1** and **2**. This assumption is supported by the experimental data in the oxidation of 2,6-DMP and 3,5-DTBC (tables 3 and 4). Though the exact value of redox potentials of each complex are unknown and their tyrosinase activities are also not very high, the result suggests that

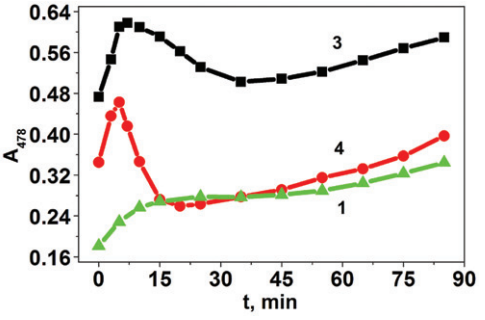


Figure 6. The oxidation of 2,6-DMP catalyzed by **1**, **3**, and **4** monitored at 478 nm as a function of reaction time. [complex] = 0.1 mmol $L^{-1}$; [2,6-DMP] = 100 mmol $L^{-1}$.



the redox potential of the metal center is a critical factor to modulate the polyphenol oxidase activity of metal complexes. For **4**, manganese is in +2 oxidation state, thus is not comparable in this case.

Oxidation of 2,6-DMP catalyzed by **1**, **3**, and **4** proceeded in three phases, as monitored at 478 nm (the absorbance of the product). At first, the absorbance increased, then started to decrease, and finally recovered gradually, as shown in figure 6. When **3** and **4** were used, the decreasing phase is more obvious. The decrease in the product absorbance suggested that the product may be converted to other transient intermediates [35–38]. However, attempts to trap the intermediates failed. It is possible that a substrate–catalyst adduct was initially formed and exhibits absorbance at the same wavelength as the product. At the beginning of reaction, the adduct formation is much faster, thus an increase in absorbance was observed. With the reaction progressing, the substrate–catalyst adduct breaks down resulting in decrease of the absorption. At the same time, the product starts to form leading to absorption recovery. The slower initial growth phase of the reaction agrees with the higher $K_m$ of **1**, suggesting that the affinity of the substrate to **1** is lower than that of **3** and **4**. Formation of 3,3′,5,5′-tetramethoxy4,4′-diphenoquinone (DPQ) identified by NMR spectroscopy (data not shown) suggests that during catalytic reactions with **1**, **3**, and **4**, a benzoquinone radical formed first, which further reacted with DMP, and DPQ was formed [39]. For 3,5-DTBC, the initial phase is probably faster, and continuously increasing kinetic curves were observed, as shown in figure S5.

Comparing tables 3 and 4, the catalytic activities of **1**, **3**, and **4** in the oxidation of 3,5-DTBC are apparently much higher than that to 2,6-DMP. The reason may be related to the structure of the substrates. The two methoxy groups on both sides of the phenolic hydroxyl group in 2,6-DMP are unfavorable for its binding to metal complex. While in 3,5-DTBC, two tert-butyl substitutions are at the 3 and 5 positions of the phenol ring, far from the hydroxyl group, thus less effective.

## 4. Conclusions

Four metal complexes with the same ligand were synthesized and structurally characterized. Their catechol oxidase and tyrosinase activities were investigated using

3,5-DTBC and 2,6-DMP as substrates, respectively. The results show that with a similar coordination sphere, iron complex **3** exhibits higher polyphenol oxidase activity than copper complexes **1** and **2**, and manganese complex **4**, because the reduction potential of the iron center is higher. The results suggest that redox potential of the metal center is a critical factor to modulate catechol oxidase and tyrosinase activities of the metal complexes.

## Supplementary material

CCDC 833277 contains the supplementary crystallographic data for **1**. These data can be obtained free of charge *via* http://www.ccdc.cam.ac.uk/conts/retrieving.html, or from the Cambridge Crystallographic Data Centre, 12 Union Road, Cambridge CB2 1EZ, UK; Fax: (+44) 1223-336-033; or Email: deposit@ccdc.cam.ac.uk

Proposed structures of **2**–**4**; Lineweaver–Burk plots for the catalytic reaction catalyzed by **1**–**4**; the oxidation of 2,6-DMP in different solvents by **2** in different solvents for different time; the time course of the oxidation reaction of 3,5-DTBC (100 mmol $L^{-1}$) catalyzed by **4**; selected IR data (in $cm^{-1}$) for four metal complexes are provided in figures S1–S5 and table S1.



## Acknowledgments

The authors gratefully acknowledge the financial support by the National Natural Science Foundation (Nos 31070742 and 21001044) and the State Key Laboratory of Bioreactor Engineering (No. 2060204).

## References

[1] R. van Gorkum, J. Berding, D.M. Tooke, A.L. Spek, J. Reedijk, E. Bouwman. *J. Catal.*, **252**, 110 (2007).
[2] K.S. Banu, T. Chattopadhyay, A. Banerjee, S. Bhattacharya, E. Suresh, M. Nethaji, E. Zangrando, D. Das. *Inorg. Chem.*, **47**, 7083 (2008).
[3] K.S. Banu, T. Chattopadhyay, A. Banerjee, M. Mukherjee, S. Bhattacharya, G.K. Patra, E. Zangrando, D. Das. *Dalton Trans.*, 8755 (2009).
[4] L. Casella, E. Monzani, M. Gullotti, D. Cavagnino, G. Cerina, L. Santagostini, R. Ugo. *Inorg. Chem.*, **35**, 7516 (1996).
[5] S. Torelli, C. Belle, S. Hamman, J.-L. Pierre, E. Saint-Aman. *Inorg. Chem.*, **41**, 3983 (2002).
[6] D.A. Rockcliffe, A.E. Martell. *J. Mol. Catal. A: Chem.*, **99**, 101 (1995).
[7] F.P.W. Agterberg, H.A.J. ProvóKluit, W.L. Driessen, J. Reedijk, H. Oevering, W. Buijs, N. Veldman, M.T. Lakin, A.L. Spek. *Inorg. Chim. Acta*, **267**, 183 (1998).
[8] R. Than, A.A. Feldmann, B. Krebs. *Coord. Chem. Rev.*, **182**, 211 (1999).
[9] C. Fernandes, A. Neves, A.J. Bortoluzzi, A.S. Mangrich, E. Rentschler, B. Szpoganicz, E. Schwingel. *Inorg. Chim. Acta*, **320**, 12 (2001).
[10] G.A. van Albada, I. Mutikainen, I. Riggio, U. Turpeinen, J. Reedijk. *Polyhedron*, **21**, 141 (2002).
[11] Y. Hitomi, A. Ando, H. Matsui, T. Ito, T. Tanaka, S. Ogo, T. Funabiki. *Inorg. Chem.*, **44**, 3473 (2005).
[12] J.-H. Qiu, Z.-R. Liao, X.-G. Meng, L. Zhu, Z.-M. Wang, K.-B. Yu. *Polyhedron*, **24**, 1617 (2005).
[13] S. Youngme, C. Chailuecha, G.A. van Albada, C. Pakawatchai, N. Chaichit, J. Reedijk. *Inorg. Chim. Acta*, **358**, 1068 (2005).

[14] J.A. Zazo, J.A. Casas, A.F. Mohedano, M.A. Gilarranz, J.J. Rodríguez. *Environ. Sci. Technol.*, **39**, 9295 (2005).
[15] A. Ray, S. Banerjee, R.J. Butcher, C. Desplanches, S. Mitra. *Polyhedron*, **27**, 2409 (2008).
[16] D. Maiti, H.R. Lucas, A.A.N. Sarjeant, K.D. Karlin. *J. Am. Chem. Soc.*, **129**, 6998 (2007).
[17] P. Haack, C. Limberg, K. Ray, B. Braun, U. Kuhlmann, P. Hildebrandt, C. Herwig. *Inorg. Chem.*, **50**, 2133 (2011).
[18] P.S. Verma, R.C. Saxena, A. Jayaraman. *Fresenius J. Anal. Chem.*, **357**, 56 (1997).
[19] F. Gloaguen, J.D. Lawrence, T.B. Rauchfuss. *J. Am. Chem. Soc.*, **123**, 9476 (2001).
[20] F.A. Garner, H.R. Brager, D.S. Gelles, J.M. McCarthy. *J. Nucl. Mater.*, **148**, 294 (1987).
[21] U.P. Singh, R. Singh, S. Hikichi, M. Akita, Y. Moro-oka. *Inorg. Chim. Acta*, **310**, 273 (2000).
[22] Y. Gultneh, Y.T. Tesema, B. Ahvazi, T.B. Yisgedu, R.J. Butcher, J.P. Tuchagues. *Inorg. Chim. Acta*, **359**, 4463 (2006).
[23] S.G. Sreerama, A. Mukhopadhyay, S. Pal. *Polyhedron*, **26**, 4101 (2007).
[24] A.A. Costa, G.F. Ghesti, J.L. de Macedo, V.S. Braga, M.M. Santos, J.A. Dias, S.C.L. Dias. *J. Mol. Catal. A: Chem.*, **282**, 149 (2008).
[25] K.S. Banu, T. Chattopadhyay, A. Banerjee, S. Bhattacharya, E. Zangrando, D. Das. *J. Mol. Catal. A: Chem.*, **310**, 34 (2009).
[26] A. Allam, I. Dechamps-Olivier, J.-B. Behr, L. Dupont, R. Plantier-Royon. *Inorg. Chim. Acta*, **366**, 310 (2011).
[27] M. Sarkar, R. Clérac, C. Mathonière, N.G.R. Hearns, V. Bertolasi, D. Ray. *Inorg. Chem.*, **49**, 6575 (2010).
[28] W.J. Geary. *Coord. Chem. Rev.*, **7**, 81 (1971).
[29] B. Karthikeyan. *Spectrochim. Acta Part A: Mol. Biomol. Spectrosc.*, **66**, 860 (2007).
[30] L. Liu, C. Liu, X. Wang, Z.G. Hu, R.K. Li, C.T. Chen. *Solid State Sci.*, **11**, 841 (2009).
[31] Z. Wang, X. Fan, D. Li, L. Feng. *Spectrochim. Acta Part A: Mol. Biomol. Spectrosc.*, **71**, 1224 (2008).
[32] S.H. Mashraqui, M. Chandiramani, R. Betkar, S. Ghorpade. *Sensors Actuators B: Chem.*, **150**, 574 (2010).
[33] W.J. Barreto, S. Ponzoni, P. Sassi. *Spectrochim. Acta Part A: Mol. Biomol. Spectrosc.*, **55**, 65 (1998).
[34] F.A. Cotton, G. Wilkinson, C.A. Murillo, M. Bochmann. *Advanced Inorganic Chemistry*, Wiley, New York (1999).
[35] C. Policar, I. Artaud, D. Mansuy. *Inorg. Chem.*, **35**, 210 (1996).
[36] J. Kaizer, G. Baráth, R. Csonka, G. Speier, L. Korecz, A. Rockenbauer, L. Párkányi. *J. Inorg. Biochem.*, **102**, 773 (2008).
[37] T. Csay, B. Kripli, M. Giorgi, J. Kaizer, G. Speier. *Inorg. Chem. Commun.*, **13**, 227 (2010).
[38] L. Ye, D. Spiteller, R. Ullrich, W. Boland, J.r. Nuüske, G. Diekert. *Biochemistry*, **49**, 7264 (2010).
[39] M.A. El-Sayed, H.A. El-Wakil, T.S. Kassem, H.A. Abo-Eldahab, A.E. El-Kholy. *Inorg. Chim. Acta*, **359**, 4304 (2006).